

Chaos Synchronization of an Electrostatic MEMS Resonator in the Presence of Parametric Uncertainties

Alexander Jimenez-Triana, Guchuan Zhu, and Lahcen Saydy

Abstract—This paper addresses the synchronization control problem of a class of chaotic systems. The synchronization is obtained by using an adaptive control law, which guarantees a global asymptotical convergence of the error between the outputs of driving and response systems in the presence of parametric uncertainties in both systems. The method of synchronization can be applied to a wide class of systems though the present work focuses only on a particular case, mainly, Micro Electro Mechanical Systems (MEMS). As an example of application, an electrostatic MEMS resonator with unknown damping and stiffness actions is synchronized with a Duffing chaotic oscillator and a MEMS chaotic oscillator. This component can be used in such applications as secure communication. Numerical simulations are carried out to confirm the validity of the developed control schemes.

I. INTRODUCTION

Chaos synchronization [1] is a phenomenon which may occur when a chaotic system drives another one by coupling them in a correct way and ensuring that both systems evolve in synchrony. Since the pioneering work of [2], a lot of research has been conducted concerning chaos synchronization, which is nowadays a widely understood phenomenon and an active topic of research [3].

Chaos synchronization is important in many fields, including biology, nonlinear optics, fluid dynamics, and electronics [1]. In particular, it finds applications in secure communications, where different methods have been developed to encode data in a chaotic signal. One of the methods consists in using a chaotic driving system to produce a chaotic carrier modulated by a message conforming the transmitter. The receiver includes a chaotic response system synchronized with the driver, in such a way that a replica of the chaotic carrier can be obtained in the receiver, and the message can be decoded by subtracting the “chaotic” part of the signal.

This standard application of chaos synchronization has motivated a great deal of research activity and many methods have been proposed to synchronize chaotic systems, including parametric perturbations [4], adaptive control [5], [6], [7], [8], variable structure control [9], impulsive control [4], backstepping [10], H_∞ control [11], [12], and so on.

It is interesting to note that in order to apply the ideas from chaos synchronization in secure communications, the

response system does not have to be the same as the driving system [5], [6], [7], [8], or as we note in the results of this paper, it does not have to be even chaotic. To obtain their results, many works using chaos synchronization and claiming applications in secure communications do not use the fact that the response system should be chaotic. However, it is common that assumptions on the dynamics of the system or its structure, such as boundedness of the solutions and Lipschitz conditions, should be easy to fulfil if the response system is chaotic since it evolves over time into a strange attractor [13].

In this paper, an algorithm to synchronize two systems is given, one of which, the driving system, is chaotic. The response system can be chaotic or not, can have the same form as the driving system, or can even be structurally different. In order to apply this idea, affine control systems are considered.

Many MEMS devices exhibit chaotic behavior in certain operational conditions [14], [15], [16], [17]. These MEMS can be seen as chaotic capacitors, which can be used, for instance, in the transmitter or the receiver circuitry in secure communication schemes using chaos [18]. In addition, as have been observed in recent results concerning the improvement of the output energy in oscillators using MEMS [19], controlling MEMS in chaotic mode can be useful to increase the amplitude of the periodic oscillations of these systems. Therefore, introducing chaos in MEMS by synchronizing them with a chaotic system can also be useful in improving the performance of different systems in which an accurate control of amplitude of oscillation is mandatory.

The organization of the rest of the paper is as follows. In Section II the dynamic of a chaotic MEMS actuator is briefly explained based on a model given in [20], [14]. Next, in Section III, the synchronization scheme using adaptive control is explained in details. Section IV presents two case studies along with the simulation results. Finally, conclusions are given in Section V.

II. DYNAMICS OF A CHAOTIC MEMS ACTUATOR

The chaotic MEMS model used in this study is presented in Fig. 1, which is taken from [20], [14]. The MEMS is modeled by a nonlinear mass-spring-damper system with external electrostatic actuation expressed as

$$m\ddot{z} + b\dot{z} + c_1z + c_3z^3 = F, \quad (1)$$

where m is the mass of the movable structure, b is the damping constant, c_1 and c_3 are the linear and cubic stiffness

A. Jimenez-Triana is with the Department of Control Engineering, Universidad Distrital Francisco José de Caldas, Cll 74 Sur No. 68A - 20, Bogotá, Colombia (e-mail: ajimenezt2@udistrital.edu.co).

G. Zhu and L. Saydy are with the Electrical Engineering Department, École Polytechnique de Montréal, Montréal, QC H3C 3A7, Canada (e-mail: guchuan.zhu@polymtl.ca, lahcen.saydy@polymtl.ca).

Manuscript received April 6, 2011.

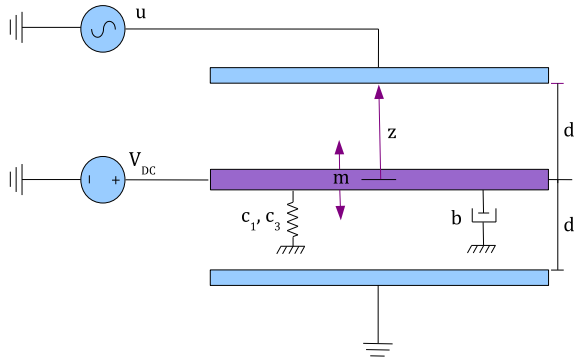


Fig. 1. Schematic of the electrostatically actuated MEMS.

coefficients, respectively, and F is the electrostatic actuation force given by

$$F = \frac{1}{2} \frac{C_0 d}{(d-z)^2} (V_{DC} + u)^2 - \frac{1}{2} \frac{C_0 d}{(d+z)^2} V_{DC}^2. \quad (2)$$

In (2) C_0 is the capacitance of the actuator at rest, which has an initial gap d between the plates and the resonator. The input voltage $V_i = (V_{DC} + u)$ is applied as shown in Fig. 1, and has two components: a DC voltage V_{DC} and a forcing voltage u , which is the actual control signal. Note that in the present work, we ignore the dynamics of the driving circuit by assuming that they are much faster than that of the mechanical structure. Note also that for simplicity, we do not take into account contact dynamics. This means that the system should operate in such a way that the moveable and fixed plates will not come into contact.

For the sake of simplicity in control design and analysis, it is convenient to describe the system dynamics in normalized coordinates [21]. We introduce then the following dimensionless variables:

$$\begin{aligned} \tau = \omega_0 t, \quad \omega = \frac{\Omega}{\omega_0}, \quad x = \frac{z}{d}, \quad \mu = \frac{b}{m\omega_0}, \quad \sigma = \frac{c_1}{m\omega_0^2}, \\ \eta = \frac{c_3 d^2}{m\omega_0^2}, \quad \gamma = \frac{C_0 V_{DC}^2}{2m\omega_0^2 d^3}, \quad A = 2\gamma \frac{1}{V_{DC}}, \quad Au = u', \end{aligned}$$

where ω_0 is the natural frequency defined by $\omega_0 = \sqrt{c_1/m}$.

In the normalized coordinates, by assuming that the DC voltage V_{DC} is much higher than the forcing voltage u , the nondimensional equation of motion becomes

$$\ddot{x} + \mu\dot{x} + \sigma x + \eta x^3 = \gamma \left(\frac{1}{(1-x)^2} - \frac{1}{(1+x)^2} \right) + \frac{u'}{(1-x)^2}. \quad (3)$$

System (3) behaves chaotically by selecting $u = V_{AC} \sin(\omega t)$, and the set of parameters $AV_{AC} = 0.04$, $\omega = 0.5$, $\gamma = 0.338$, $\mu = 0.01$, $\sigma = 1$, and $\eta = 12$, as may be observed in the phase diagram of Fig. 2 and the Lyapunov exponents diagram of Fig. 3. The existence of one positive Lyapunov exponent confirms the chaotic behavior of the system.

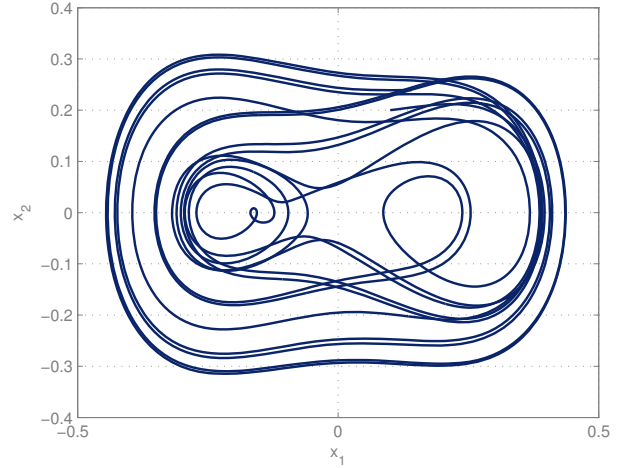


Fig. 2. State space evolution for the system (3) with the set of parameters $\gamma = 0.338$, $AV_{AC} = 0.04$, $\omega = 0.5$, $\sigma = 1$, $\mu = 0.01$, and $\eta = 12$.

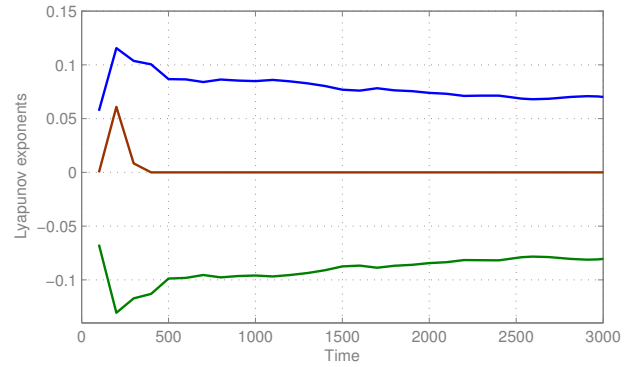


Fig. 3. Lyapunov exponents for the system (3) with the set of parameters: $\gamma = 0.338$, $AV_{AC} = 0.04$, $\omega = 0.5$, $\sigma = 1$, $\mu = 0.01$, and $\eta = 12$.

III. SYNCHRONIZATION OF AFFINE CHAOTIC SYSTEMS

Consider a class of two-dimensional uncertain chaotic system

$$\dot{\mathbf{x}} = \mathbf{F}(\mathbf{x}) \boldsymbol{\alpha} + \mathbf{f}(t, \mathbf{x}) \quad (4)$$

which is named the driving or master system, and

$$\dot{\mathbf{y}} = \mathbf{G}(\mathbf{y}) \boldsymbol{\beta} + \mathbf{g}(t, \mathbf{y}) + \mathbf{h}(\mathbf{y}) u \quad (5)$$

which is named the response or slave system, where $\mathbf{x} = (x_1 \ x_2)^T \in \mathbb{R}^2$ and $\mathbf{y} = (y_1 \ y_2)^T \in \mathbb{R}^2$ are bounded state vectors, $\boldsymbol{\alpha} = (\alpha_1 \ \alpha_2 \ \dots \ \alpha_n)^T \in D \subset \mathbb{R}^n$, with D a subset of \mathbb{R}^n which guarantees that the driving system is chaotic, and $\boldsymbol{\beta} = (\beta_1 \ \beta_2 \ \dots \ \beta_p)^T \in \mathbb{R}^p$ are uncertain parameters, $\mathbf{F}(\mathbf{x}) : \mathbb{R}^2 \rightarrow \mathbb{R}^2 \times \mathbb{R}^n$ and $\mathbf{G}(\mathbf{y}) : \mathbb{R}^2 \rightarrow \mathbb{R}^2 \times \mathbb{R}^p$ are matrices defined by

$$\begin{aligned} \mathbf{F}(\mathbf{x}) &= \begin{bmatrix} 0 & 0 & \dots & 0 \\ F_{21}(\mathbf{x}) & F_{22}(\mathbf{x}) & \dots & F_{2n}(\mathbf{x}) \end{bmatrix} = \begin{bmatrix} \mathbf{0} \\ \mathbf{F}_2 \end{bmatrix} \\ \mathbf{G}(\mathbf{y}) &= \begin{bmatrix} 0 & 0 & \dots & 0 \\ G_{21}(\mathbf{y}) & G_{22}(\mathbf{y}) & \dots & G_{2p}(\mathbf{y}) \end{bmatrix} = \begin{bmatrix} \mathbf{0} \\ \mathbf{G}_2 \end{bmatrix} \end{aligned} \quad (6)$$

$\mathbf{f}(t, \mathbf{x}) : \mathbb{R}^+ \times \mathbb{R}^2 \rightarrow \mathbb{R}^2$, $\mathbf{g}(t, \mathbf{y}) : \mathbb{R}^+ \times \mathbb{R}^2 \rightarrow \mathbb{R}^2$ and $\mathbf{h}(\mathbf{y}) : \mathbb{R}^2 \rightarrow \mathbb{R}^2$ are vectors given by

$$\mathbf{f}(t, \mathbf{x}) = \begin{bmatrix} x_2 \\ f(t, \mathbf{x}) \end{bmatrix}, \mathbf{g}(t, \mathbf{y}) = \begin{bmatrix} y_2 \\ g(t, \mathbf{y}) \end{bmatrix}, \quad (7)$$

$$\mathbf{h}(\mathbf{y}) = [0 \quad h_2(\mathbf{y})]^T, \quad (8)$$

and $u(t, \mathbf{x}, \mathbf{y}) : \mathbb{R}^+ \times \mathbb{R}^2 \times \mathbb{R}^2 \rightarrow \mathbb{R}$ is a scalar control input. We suppose that $\mathbf{F}(\mathbf{x})$, $\mathbf{f}(t, \mathbf{x})$, $\mathbf{G}(\mathbf{y})$, $\mathbf{g}(t, \mathbf{y})$, and $\mathbf{h}(\mathbf{y})$ satisfy some regularity conditions, such as Lipschitz continuity, to ensure, e.g., the existence and the uniqueness of solutions of systems (4) and (5).

The control objective is to design a state feedback control u such that the states of the response system, \mathbf{y} , asymptotically track that of the driving system, \mathbf{x} , or equivalently, the response system synchronizes the driving system. To this end, we define the error vector by $\mathbf{e} = \mathbf{y} - \mathbf{x} = (e_1 \quad e_2)^T \in \mathbb{R}^2$ and the parameter estimation errors as $\tilde{\boldsymbol{\alpha}} = \boldsymbol{\alpha} - \hat{\boldsymbol{\alpha}}$, $\tilde{\boldsymbol{\beta}} = \boldsymbol{\beta} - \hat{\boldsymbol{\beta}}$, where $\hat{\boldsymbol{\alpha}}$, $\hat{\boldsymbol{\beta}}$ are the estimated values of $\boldsymbol{\alpha}$ and $\boldsymbol{\beta}$, respectively. The control objective can then be thought as to asymptotically stabilize the error dynamics around the origin, implying $\lim_{t \rightarrow \infty} \|\mathbf{e}\| = 0$.

Based on these definitions, one can assert the following result.

Theorem 1: For given positive constants k_1 , k_2 , γ_1 , and γ_2 , if the control input u is given by

$$u = h_2^{-1}(\mathbf{y}) \left(-\mathbf{G}_2 \hat{\boldsymbol{\beta}} + \mathbf{F}_2 \hat{\boldsymbol{\alpha}} - g(t, \mathbf{y}) + f(t, \mathbf{x}) - k_2^{-1} (k_1 e_1 + k_2 e_2) - k_2^{-1} k_1 e_2 \right), \quad (9)$$

and the parameters are updated according to the laws

$$\begin{aligned} \dot{\hat{\boldsymbol{\alpha}}}^T &= -\gamma_1 (k_1 e_1 + k_2 e_2) k_2 \mathbf{F}_2, \\ \dot{\hat{\boldsymbol{\beta}}}^T &= \gamma_2 (k_1 e_1 + k_2 e_2) k_2 \mathbf{G}_2, \end{aligned} \quad (10)$$

then the response system (5) synchronizes the driving system (4) globally and asymptotically.

Proof: It can be derived from (4) and (5) that the synchronization error dynamics are given by

$$\dot{\mathbf{e}} = \dot{\mathbf{y}} - \dot{\mathbf{x}} = \mathbf{G}(\mathbf{y}) \boldsymbol{\beta} + \mathbf{g}(t, \mathbf{y}) + \mathbf{h}(\mathbf{y}) u(t, \mathbf{x}, \mathbf{y}) - \mathbf{F}(\mathbf{x}) \boldsymbol{\alpha} - \mathbf{f}(t, \mathbf{x}). \quad (11)$$

The derivatives of the parameter estimation errors are

$$\begin{aligned} \dot{\tilde{\boldsymbol{\alpha}}} &= -\dot{\hat{\boldsymbol{\alpha}}}, \\ \dot{\tilde{\boldsymbol{\beta}}} &= -\dot{\hat{\boldsymbol{\beta}}}. \end{aligned} \quad (12)$$

By defining the following Lyapunov function candidate:

$$V(\mathbf{e}, \tilde{\boldsymbol{\alpha}}, \tilde{\boldsymbol{\beta}}) = \frac{1}{2} \left((k_1 e_1 + k_2 e_2)^2 + 2k_1 k_2 e_1^2 + \frac{1}{\gamma_1} \tilde{\boldsymbol{\alpha}}^T \tilde{\boldsymbol{\alpha}} + \frac{1}{\gamma_2} \tilde{\boldsymbol{\beta}}^T \tilde{\boldsymbol{\beta}} \right), \quad (13)$$

and taking its time derivative, one obtains

$$\begin{aligned} \dot{V}(\mathbf{e}, \tilde{\boldsymbol{\alpha}}, \tilde{\boldsymbol{\beta}}) &= (k_1 e_1 + k_2 e_2) (k_1 \dot{e}_1 + k_2 \dot{e}_2) \\ &\quad + 2k_1 k_2 e_1 \dot{e}_1 + \frac{1}{\gamma_1} \tilde{\boldsymbol{\alpha}}^T \dot{\tilde{\boldsymbol{\alpha}}} + \frac{1}{\gamma_2} \tilde{\boldsymbol{\beta}}^T \dot{\tilde{\boldsymbol{\beta}}} \\ &= (k_1 e_1 + k_2 e_2) [k_2 \mathbf{G}_2 \tilde{\boldsymbol{\beta}} - k_2 \mathbf{F}_2 \tilde{\boldsymbol{\alpha}} \\ &\quad + k_2 h_2(\mathbf{y}) u(t, \mathbf{x}, \mathbf{y}) + k_2 g(t, \mathbf{y}) - k_2 f(t, \mathbf{x}) \\ &\quad + k_1 e_2] + 2k_1 k_2 e_1 e_2 - \frac{1}{\gamma_1} \tilde{\boldsymbol{\alpha}}^T \dot{\tilde{\boldsymbol{\alpha}}} - \frac{1}{\gamma_2} \tilde{\boldsymbol{\beta}}^T \dot{\tilde{\boldsymbol{\beta}}} \\ &= (k_1 e_1 + k_2 e_2) k_2 \mathbf{G}_2 \tilde{\boldsymbol{\beta}} - (k_1 e_1 + k_2 e_2) k_2 \mathbf{F}_2 \tilde{\boldsymbol{\alpha}} \\ &\quad - (k_1 e_1 + k_2 e_2)^2 + 2k_1 k_2 e_1 e_2 - \frac{1}{\gamma_1} \tilde{\boldsymbol{\alpha}}^T \dot{\tilde{\boldsymbol{\alpha}}} \\ &\quad - \frac{1}{\gamma_2} \tilde{\boldsymbol{\beta}}^T \dot{\tilde{\boldsymbol{\beta}}}, \end{aligned} \quad (14)$$

which can be written as

$$\begin{aligned} \dot{V}(\mathbf{e}, \tilde{\boldsymbol{\alpha}}, \tilde{\boldsymbol{\beta}}) &= - \left(\frac{1}{\gamma_1} \dot{\tilde{\boldsymbol{\alpha}}}^T + (k_1 e_1 + k_2 e_2) k_2 \mathbf{F}_2 \right) \tilde{\boldsymbol{\alpha}} \\ &\quad - \left(\frac{1}{\gamma_2} \dot{\tilde{\boldsymbol{\beta}}}^T - (k_1 e_1 + k_2 e_2) k_2 \mathbf{G}_2 \right) \tilde{\boldsymbol{\beta}} \\ &\quad - k_1^2 e_1^2 - k_2^2 e_2^2. \end{aligned} \quad (15)$$

By replacing (10) into (15), one obtains

$$\dot{V}(\mathbf{e}, \tilde{\boldsymbol{\alpha}}, \tilde{\boldsymbol{\beta}}) = -k_1^2 e_1^2 - k_2^2 e_2^2 \leq 0, \quad (16)$$

which is negative semi-definite. Then we conclude that $V(\mathbf{e}, \tilde{\boldsymbol{\alpha}}, \tilde{\boldsymbol{\beta}}) \leq V(0)$ and the error dynamics are stable. Noting that with the control given in (9) the synchronization error dynamics are autonomous, we can apply LaSalle's invariance theorem to show the asymptotic stability of the error dynamics. To this end, we consider the set $E = \{(e_1, e_2) \in \mathbb{R}^2 \mid \dot{V} = 0\}$. Since the equilibrium point of the error dynamics ($e_1 = 0, e_2 = 0$) is the unique invariant set in E , we can conclude that $\lim_{t \rightarrow \infty} \|\mathbf{e}\| = 0$. Hence (5) follows (4) globally and asymptotically, which completes the proof. \blacksquare

IV. CHAOS SYNCHRONIZATION OF MEMS RESONATOR AND SIMULATION VALIDATION

The synchronization method presented above can be applied to a great variety of systems, such as Duffing, Helmholtz, pendulum, MEMS, and many other chaotic oscillators. In order to confirm the generality of the developed method, we apply it firstly to synchronize two structurally different systems: a chaotic Duffing system and a non chaotic MEMS. Then we will apply this method to synchronize two structurally similar systems, a chaotic MEMS with a non chaotic one.

A. Synchronizing a chaotic Duffing System with a MEMS

In this example, the driving system is a Duffing system and the response system is the MEMS described in the Sect. II with a control input u .

We consider uncertainties in the parameters of the driving and response systems for which the damping factor as well as the linear and cubic nonlinear stiffness coefficients are unknown constants.

The Duffing system is given by

$$\ddot{x} = -\alpha_1 x - \alpha_2 \dot{x} - \alpha_3 x^3 + A \cos(\omega t), \quad (17)$$

which is chaotic for the set of parameters $\alpha_1 = -1.1$, $\alpha_2 = 0.4$, $\alpha_3 = 25$, $A = 0.42$, and $\omega = 1.8$. This system can be written in the form of (4), by defining the state variables x_1 and x_2 as follows

$$\begin{bmatrix} \dot{x}_1 \\ \dot{x}_2 \end{bmatrix} = \begin{bmatrix} 0 & 0 & 0 \\ -x_1 & -x_2 & -x_1^3 \end{bmatrix} \begin{bmatrix} \alpha_1 \\ \alpha_2 \\ \alpha_3 \end{bmatrix} + \begin{bmatrix} x_2 \\ A \cos(\omega t) \end{bmatrix}. \quad (18)$$

In a similar way, the response system is given by

$$\begin{aligned} & \ddot{y} + \beta_1 y + \beta_2 \dot{y} + \beta_3 y^3 \\ & = \gamma \left(\frac{1}{(1-y)^2} - \frac{1}{(1+y)^2} \right) + \frac{u}{(1-y)^2} \end{aligned} \quad (19)$$

and can be written in the form of (5), by taking

$$\begin{aligned} \begin{bmatrix} \dot{y}_1 \\ \dot{y}_2 \end{bmatrix} &= \begin{bmatrix} 0 & 0 & 0 \\ -y_1 & -y_2 & -y_1^3 \end{bmatrix} \begin{bmatrix} \beta_1 \\ \beta_2 \\ \beta_3 \end{bmatrix} + \begin{bmatrix} y_2 \\ g_1(\mathbf{y}, t) \end{bmatrix} \\ &+ \begin{bmatrix} 0 \\ \frac{1}{(1-y)^2} \end{bmatrix}^T u \end{aligned} \quad (20)$$

with $g_1(\mathbf{y}, t)$ given by

$$g_1(\mathbf{y}, t) = \gamma \left(\frac{1}{(1-y_1)^2} - \frac{1}{(1+y_1)^2} \right). \quad (21)$$

The control objective is to design a control u such that the states (y_1, y_2) track asymptotically the states (x_1, x_2) . The matrices $\mathbf{F}(\mathbf{x})$, $\mathbf{G}(\mathbf{y})$ and the vectors $\mathbf{f}(\mathbf{x}, t)$, $\mathbf{g}(\mathbf{y}, t)$, and $\mathbf{h}(\mathbf{y})$ are of the form

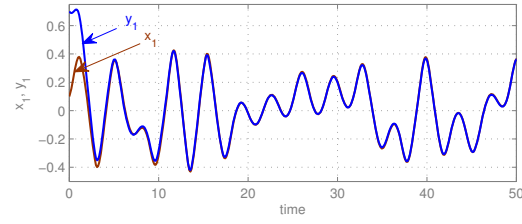
$$\begin{aligned} \mathbf{F}(\mathbf{x}) &= \begin{bmatrix} 0 & 0 & 0 \\ -x_1 & -x_2 & -x_1^3 \end{bmatrix} = \begin{bmatrix} 0 \\ \mathbf{F}_2 \end{bmatrix}, \\ \mathbf{G}(\mathbf{y}) &= \begin{bmatrix} 0 & 0 & 0 \\ -y_1 & -y_2 & -y_1^3 \end{bmatrix} = \begin{bmatrix} 0 \\ \mathbf{G}_2 \end{bmatrix}, \\ \mathbf{f}(\mathbf{x}, t) &= \begin{bmatrix} x_2 \\ A \cos(\omega t) \end{bmatrix}, \quad \mathbf{g}(\mathbf{y}, t) = \begin{bmatrix} y_2 \\ g_1(\mathbf{y}, t) \end{bmatrix}, \\ \mathbf{h}(\mathbf{y}) &= \begin{bmatrix} 0 \\ \frac{1}{(1-y)^2} \end{bmatrix}^T. \end{aligned}$$

Based on Theorem 1, the control signal is given by

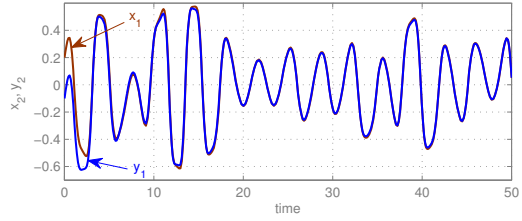
$$\begin{aligned} u_3 &= (1-y)^2 \left(y_1 \hat{\beta}_1 + y_2 \hat{\beta}_2 + y_1^3 \hat{\beta}_3 - x_1 \hat{\alpha}_1 \right. \\ &\quad \left. - x_2 \hat{\alpha}_2 - x_1^3 \hat{\alpha}_3 - g_1 + A \cos(\omega t) \right. \\ &\quad \left. - k_2^{-1} (k_1 e_1 + k_2 e_2) - k_2^{-1} k_1 e_2 \right) \end{aligned} \quad (22)$$

where the parameters are updated by the laws

$$\begin{aligned} \dot{\hat{\alpha}}^T &= -\gamma_1 (k_1 e_1 + k_2 e_2) k_2 \mathbf{F}_2 \\ &= -\gamma_1 (k_1 e_1 + k_2 e_2) k_2 \begin{bmatrix} -x_1 & -x_2 & -x_1^3 \end{bmatrix}, \end{aligned} \quad (23)$$

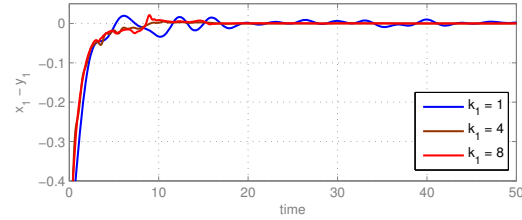


(a)

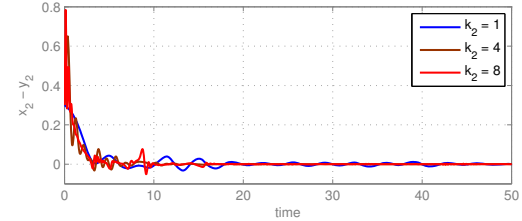


(b)

Fig. 4. Trajectories of the synchronized systems (18) and (20) with control gains $k_1 = k_2 = 1$: (a) (x_1, y_1) ; (b) (x_2, y_2) .



(a)



(b)

Fig. 5. Error signals for the synchronized systems (18) and (20): (a) error between the states (x_1, y_1) ; (b) error between the states (x_2, y_2) .

$$\begin{aligned} \dot{\hat{\beta}}^T &= \gamma_2 (k_1 e_1 + k_2 e_2) k_2 \mathbf{G}_2 \\ &= \gamma_2 (k_1 e_1 + k_2 e_2) k_2 \begin{bmatrix} -y_1 & -y_2 & -y_1^3 \end{bmatrix}. \end{aligned} \quad (24)$$

In this way, the error can be asymptotically diminished and the response system synchronizes the driving one. Figure 4 shows the trajectories of x_1, y_1 , and x_2, y_2 , from which we can observe how the systems evolve in synchrony for gains $k_1 = 1$ and $k_2 = 1$. For higher values of the gains, the simulation shows a better agreement between the signals. In Fig. 5, the evolution of the errors for different gains can be observed. It is shown how the errors diminish whatever the gain be, although they decrease faster when the gain increases. Figure 6 illustrates the evolution of α and β parameters and shows how they tends to a bounded stationary value.

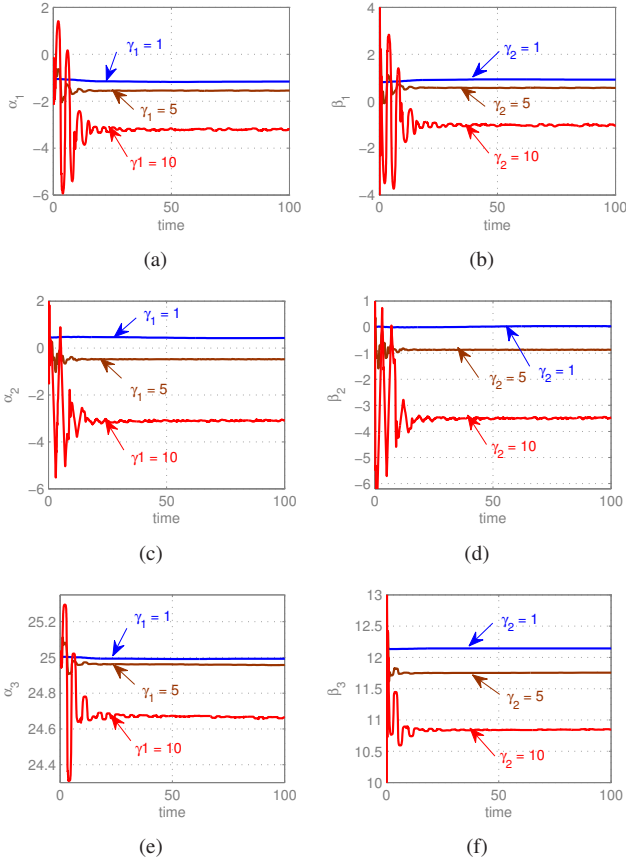


Fig. 6. Estimation of the parameters: (a) α_1 ; (b) β_1 ; (c) α_2 ; (d) β_2 ; (e) α_3 ; (f) β_3 .

B. Synchronization of two chaotic and non chaotic MEMS

In this example, the driving system is the chaotic MEMS presented in Sect. II and the response system is the MEMS given by the equation (19). The driving system can be written in the form of (4)

$$\begin{bmatrix} \dot{x}_1 \\ \dot{x}_2 \end{bmatrix} = \begin{bmatrix} 0 & 0 & 0 \\ -x_1 & -x_2 & -x_1^3 \end{bmatrix} \begin{bmatrix} \alpha_1 \\ \alpha_2 \\ \alpha_3 \end{bmatrix} + \begin{bmatrix} x_2 \\ f_1(\mathbf{x}, t) \end{bmatrix} \quad (25)$$

with

$$f_1(\mathbf{x}, t) = \gamma \left(\frac{1}{(1-x_1)^2} - \frac{1}{(1+x_1)^2} \right) + \frac{A}{(1-x_1)^2} \sin(\omega t). \quad (26)$$

The response system can be written in the form of (5) as in (20), in such a way that one can apply Theorem 1 by identifying the matrices $\mathbf{F}(\mathbf{x})$, $\mathbf{G}(\mathbf{y})$ and the vectors $\mathbf{f}(\mathbf{x}, t)$, $\mathbf{g}(\mathbf{y}, t)$, and $\mathbf{h}(\mathbf{y})$ as

$$\mathbf{F}(\mathbf{x}) = \begin{bmatrix} 0 & 0 & 0 \\ -x_1 & -x_2 & -x_1^3 \end{bmatrix} = \begin{bmatrix} 0 \\ \mathbf{F}_2 \end{bmatrix},$$

$$\mathbf{G}(\mathbf{y}) = \begin{bmatrix} 0 & 0 & 0 \\ -y_1 & -y_2 & -y_1^3 \end{bmatrix} = \begin{bmatrix} 0 \\ \mathbf{G}_2 \end{bmatrix},$$

$$\mathbf{f}(\mathbf{x}, t) = \begin{bmatrix} x_2 \\ f_1(\mathbf{x}, t) \end{bmatrix}, \mathbf{g}(\mathbf{y}, t) = \begin{bmatrix} y_2 \\ g_1(\mathbf{y}, t) \end{bmatrix},$$

$$\mathbf{h}(\mathbf{y}) = \begin{bmatrix} 0 \\ \frac{1}{(1-y)^2} \end{bmatrix}^T,$$

and obtaining the following control signal

$$u_3 = (1-y)^2 \left(y_1 \hat{\beta}_1 + y_2 \hat{\beta}_2 + y_1^3 \hat{\beta}_3 - x_1 \hat{\alpha}_1 - x_2 \hat{\alpha}_2 - x_1^3 \hat{\alpha}_3 - g_1 + f_1(\mathbf{x}, t) - k_2^{-1} (k_1 e_1 + k_2 e_2) - k_2^{-1} k_1 e_2 \right) \quad (27)$$

with parameters updated by the laws

$$\begin{aligned} \dot{\hat{\alpha}}^T &= -\gamma_1 (k_1 e_1 + k_2 e_2) k_2 \mathbf{F}_2 \\ &= -\gamma_1 (k_1 e_1 + k_2 e_2) k_2 [-x_1 \quad -x_2 \quad -x_1^3], \quad (28) \\ \dot{\hat{\beta}}^T &= \gamma_2 (k_1 e_1 + k_2 e_2) k_2 \mathbf{G}_2 \\ &= \gamma_2 (k_1 e_1 + k_2 e_2) k_2 [-y_1 \quad -y_2 \quad -y_1^3]. \quad (29) \end{aligned}$$

Figure 7 shows how the systems are synchronized, with an excellent agreement between signals after a transient time. The error between the synchronized states decreases asymptotically with time, as shown in Fig. 8. The estimation of the unknown parameters α and β is given in Fig. 9.

V. CONCLUSIONS

This paper presents an adaptive control scheme for synchronization of a class of chaotic systems with parametric uncertainties. The developed method is applied to the synchronization of two structurally different systems, a Duffing system and a MEMS, and structurally similar systems, a chaotic MEMS resonator and a non-chaotic MEMS. It is confirmed that in chaotic synchronization, the response system does not have to, but can be chaotic. This is a very important property that can be used in such application as secure communication. Other advantage of synchronizing

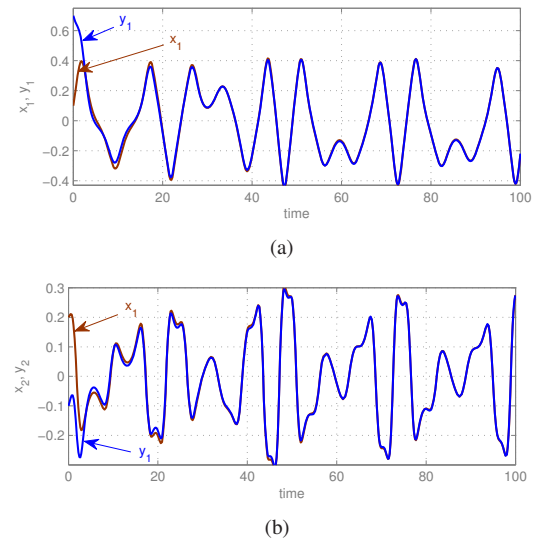


Fig. 7. Trajectories of the synchronized systems (25) and (20) with control gains $k_1 = k_2 = 1$: (a) (x_1, y_1) ; (b) (x_2, y_2) .

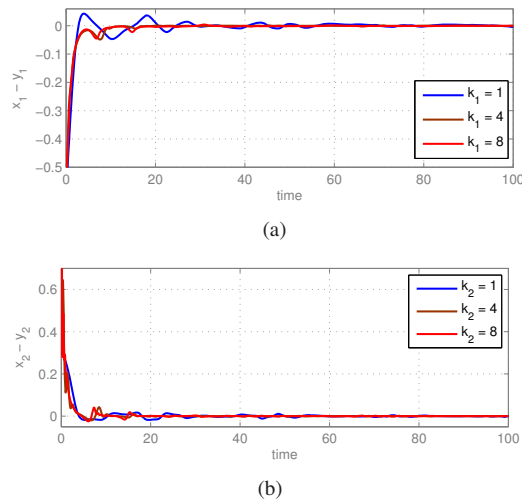


Fig. 8. Error signals for the synchronized systems (25) and (20): (a) error between (x_1, y_1) ; (b) error between (x_2, y_2) .

MEMS with a chaotic system is that this would allow an enhancement of the amplitude of the oscillation when MEMS are used as resonators and recovered from the chaotic state by controlling it. This is an important aspect for applications which require an accurate control of oscillation amplitude. Finally, it is worth noting that the scheme developed in the present work is based on state-feedback. For more realistic applications, output feedback should be considered. This issue is beyond the scope of this paper and remains an interesting topic of future work.

REFERENCES

- [1] S. Boccaletti, J. Kurths, G. Osipov, D. L. Valladares, and C. S. Zhou, "The synchronization of chaotic systems," *Physics Reports*, vol. 336, pp. 1–101, 2002.
- [2] L. M. Pecora and T. L. Carroll, "Synchronization in chaotic systems," *Physical Review Letters*, vol. 64, no. 8, pp. 821–824, 1990.
- [3] A. Loria and A. Zavala-Rio, "Adaptive tracking control of chaotic systems with applications to synchronization," *IEEE Trans. on Circuits and Systems I*, vol. 54, no. 9, pp. 1549–8358, 2007.
- [4] V. V. Astakhov, V. S. Anishchenko, T. Kapitaniak, and A. V. Shabunin, "Synchronization of chaotic oscillators by periodic parametric perturbations," *Physica D*, vol. 109, pp. 11–16, 1997.
- [5] M. T. Yassen, "Adaptive synchronization of two different uncertain chaotic systems," *Physics Letters A*, vol. 337, pp. 335–341, 2005.
- [6] H. Zhang, W. Huang, Z. Wang, and T. Chai, "Adaptive synchronization between two different chaotic systems with unknown parameters," *Physics Letters A*, vol. 350, pp. 363–366, 2006.
- [7] Y. Chang, X. Li, Y. Chu, and X. Han, "Synchronization of two physical systems with fully unknown parameters by adaptive control," in *IEEE 2009 International Workshop on Chaos-Fractals Theories and Applications*, Shenyang, 6–8 Nov. 2009, pp. 25–29.
- [8] X. Chen and J. Lu, "Adaptive synchronization of different chaotic systems with fully unknown parameters," *Physics Letters A*, vol. 364, pp. 123–128, 2007.
- [9] M. S. Tavazoei and M. Haeri, "Synchronization of chaotic fractional-order systems via active sliding mode controller," *Physics Letters A*, vol. 387, pp. 57–70, 2008.
- [10] S. Bowong and F. M. M. Kakmeni, "Synchronization of uncertain chaotic systems via backstepping approach," *Chaos, Solitons and Fractals*, vol. 21, 2004.
- [11] C. K. Ahn, S. Jung, S. Kang, and S. Joo, "Adaptive H_∞ synchronization for uncertain chaotic systems with external disturbance," *Commun Nonlinear Sci Numer Simulat*, vol. 15, pp. 2168–2177, 2010.

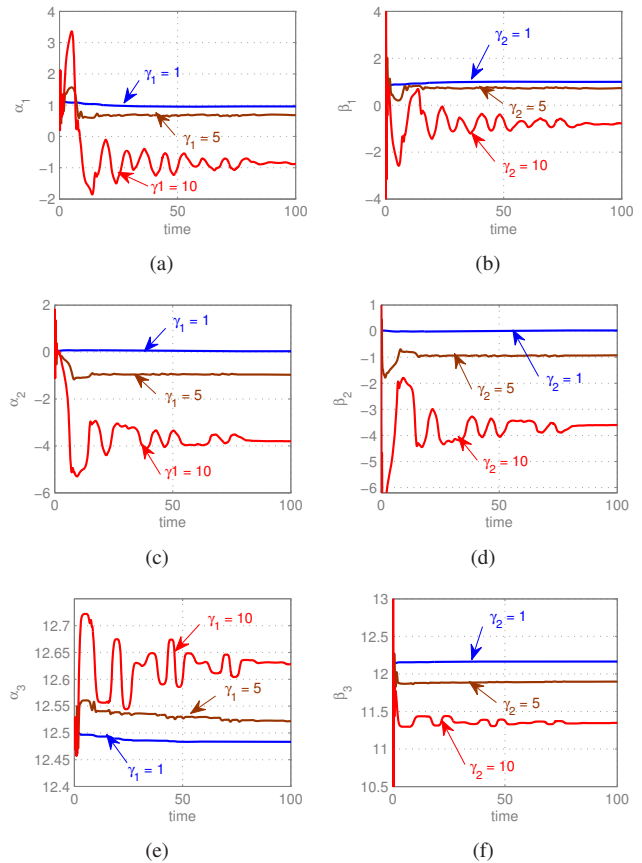


Fig. 9. Parameter estimates: (a) α_1 ; (b) β_1 ; (c) α_2 ; (d) β_2 ; (e) α_3 ; (f) β_3 .

- [12] J. A. K. Suykens, P. F. Curran, J. Vandewalle, and L. O. Chua, "Robust nonlinear H_∞ synchronization of chaotic Lur'e systems," *IEEE Trans. on Circuits and Systems I*, vol. 44, no. 10, pp. 891–904, 1997.
- [13] M. Feki, "An adaptive chaos synchronization scheme applied to secure communications," *Chaos, Solitons and Fractals*, vol. 18, pp. 141–148, 2003.
- [14] H. S. Haghghi and A. H. D. Markazi, "Chaos prediction and control in MEMS resonators," *Commun Nonlinear Sci Numer Simulat*, vol. 15, no. 10, pp. 3091–3099, 2010.
- [15] S. K. De and N. R. Aluru, "Complex oscillations and chaos in electrostatic microelectromechanical systems under superharmonic excitations," *Physical Review Letters*, vol. 94, no. 20, 2005.
- [16] S. Liu, A. Davidson, and Q. Lin, "Simulation studies on nonlinear dynamics and chaos in a MEMS cantilever control system," *J. Microelectromech. Microeng.*, vol. 14, pp. 1064–1073, 2004.
- [17] A. C. J. Luo and F. Y. Wang, "Chaotic motion in a micro-electromechanical system with non-linearity from capacitors," *Communications in Nonlinear Science and Numerical Simulation*, vol. 7, pp. 31–49, 2002.
- [18] Y. C. Wang, S. G. Adams, J. S. Thorp, N. C. MacDonald, P. Hartwell, and F. Bertsch, "Chaos in MEMS, parameter estimation and its potential application," *IEEE Trans. on Circuits and Systems I*, vol. 45, no. 10, pp. 1013–1020, 1998.
- [19] K. Park, Q. Chen, and Y.-C. Lai, "Energy enhancement and chaos control in microelectromechanical systems," *Physical Review E*, vol. 77, 2008.
- [20] R. M. C. Mestrom, R. H. B. Fey, J. T. M. van Beek, K. L. Phan, and H. Nijmeijer, "Modelling the dynamics of a MEMS resonator: simulations and experiments," *Sensors and Actuators A*, vol. 142, pp. 306–315, 2008.
- [21] J. Pont-Nin, A. Rodríguez, and L. M. Castañer, "Voltage and pull-in time in current drive of electrostatic actuators," *J. Microelectromech. Syst.*, vol. 11, no. 3, pp. 196–205, 2002.